Proceedings of the Fifth IASTED International Conference
CIRCUITS, SIGNALS, AND SYSTEMS
July 2–4, 2007, Banff, Alberta, Canada
ISBN Hardcopy: 978-0-88986-669-0 / CD: 978-0-88986-670-6

ADAPTIVE STABILIZING CONTROL OF A POWER SYSTEM THROUGH UPFC SHUNT AND SERIES CONVERTERS

A.H.M.A.Rahim
Department of Electrical Engineering
King Fahd University of Petroleum & Minerals
Dhahran, Saudi Arabia
ahrahim@kfupm.edu.sa

E.P.Nowicki
Department of Electrical and Computer Engineering
University of Calgary
Calgary, AB, Canada
enowicki@ucalgary.ca

ABSTRACT
The dynamic performance of a power system can be improved by using additional controls in a unified power flow controller (UPFC). Self-tuning adaptive control of the voltage magnitude of the series converter and phase angle of shunt converter for stabilization are considered in this article. From the input-output data record, a linear plant model of the UPFC is identified through a least square regressive algorithm. Stabilizing control is derived for the identified model through a pole-shifting technique. Simulations have been carried out for a range of operation with various disturbances. While both the controls are effective in stabilizing the system, the shunt converter phase angle control was observed to be superior. Responses were compared with optimized PI control and robustness of the proposed adaptive algorithms was tested.

KEY WORDS
Power system stabilizing control, UPFC, on-line identification, adaptive control, pole - shifting control

1. Introduction

The unified power flow controller (UPFC) is the most versatile FACTS device that has emerged for the control and optimization of power flow in electrical power transmission systems. It offers major potential advantages for the static and dynamic operation of transmission lines since it combines the features of both the Static Synchronous Compensators (STATCOM) and the Static Synchronous Series Compensator (SSSC).

The UPFC is able to control, simultaneously or selectively, all the parameters affecting power flow in the transmission line. It can also perform loop flow control, load sharing among parallel corridors, providing voltage support, enhancement of transient stability, mitigation of system oscillations, etc. [1-2]. The stability and damping control aspect of an UPFC has been investigated by a number of researchers [3-7]. Most of the control studies in power systems are based on linearized models of the nonlinear power system dynamics. The methods include exact linearization, linear quadratic regulator theory, direct feedback linearization, etc. Stabilizers based on conventional linear control theory with fixed parameters can be very well tuned to an operating condition and provide excellent damping under that condition, but they cannot provide effective control over a wide operating range for systems that are nonlinear, time varying and subject to uncertainty. Considering the above, it is desirable to develop a controller which has the ability to adjust its own parameters, finding the system structure or model on-line according to the environment in which it works to yield satisfactory control performance. Applications of adaptive control theory to excitation control problems as well as to SVC systems have been reported in the literature [8, 9]. UPFC is relatively new power electronics based device, and its control studies have generally been limited in this regard.

In this article, a UPFC controller design which identifies the model on-line and tunes the parameters of the model adaptively is proposed. The control design is based on a variable pole-shift method employing the identified system model. Performance of controls in the series as well as the parallel converters is investigated.

2. Power System Model with UPFC

Fig. 1 shows a single machine system connected to a large power system bus through a transmission line installed with UPFC. The UPFC is composed of an excitation transformer (ET), a boosting transformer (BT), two three-phase GTO based voltage source converters (VSC), and a DC link capacitor [5]. The quantities m and α in the figure refer to amplitude modulation index and phase angle of the control signal of the two voltage source converters, respectively.

Representing the synchronous generator-exciter system through a 4 differential equations, including the series and parallel transformer line dynamics, and one differential equation to represent the DC link, the composite model of a synchronous generator UPEC system can be expressed through the 9th order dynamic relationship,

$$\dot{x} = f[x,u] \qquad (1)$$

Here, the state variables are the d-q components of the shunt and series (line) currents respectively, the DC capacitor voltage, and four states from the generator-exciter system. The control vector comprises of the magnitude and phase angles of the converter voltages, $u=[m_E\ \alpha_E\ \ m_B\ \alpha_B]^T$

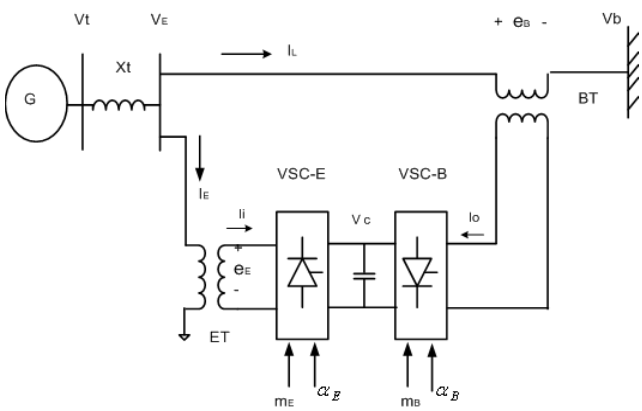

Figure 1 A single machine infinite bus system with UPFC

3. Self-tuning Adaptive Regulator

Self tuning control employs a feedback controller loop in which the controller parameters are modified depending on the error between the real plant output and the output of the plant model, as shown in Fig.2. The control for the plant is designed using a linear plant model, parameters of which are estimated and updated recursively.

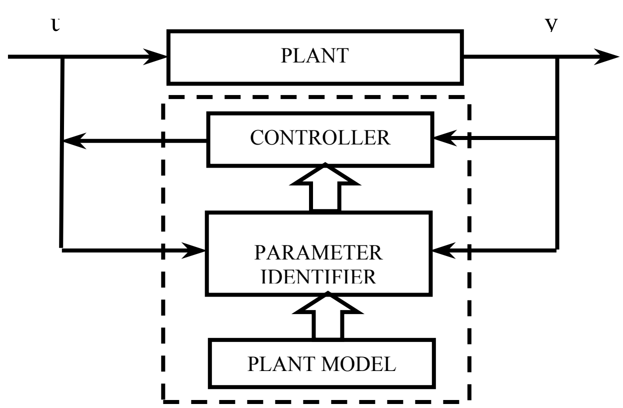

Figure 2 Block diagram of self-tuning controller

The plant model is assumed to be of the form,

$$A(z^{-1})y(t)=B(z^{-1})u(t)+e(t) \qquad (2)$$

where, $y(t)$,$u(t)$ and $e(t)$ are system output, input and the white noise, respectively; z^{-1} is the delay operator. The polynomial A and B are defined as,

$$A(z^{-1}) = 1+ a_1z^{-1} + a_2z^{-2} + a_3z^{-3} + a_4z^{-4} + \ldots\ldots\ldots\ldots \qquad (3)$$

$$B(z^{-1}) = 1+ b_1z^{-1} + b_2z^{-2} + b_3z^{-3} + b_4z^{-4} + \ldots\ldots\ldots\ldots \qquad (4)$$

The vector of parameters $\theta(t)= [a_1\ a_2\ \ldots\ldots,b_1\ b_2\ \ldots\ldots]^T$ are calculated recursively on-line through the recursive least square [8] technique using,

$$\theta(t+1) = \theta(t) +K(t)\ [y(t) – \theta^T(t)\psi(t)] \qquad (5)$$

The measurement vector, modifying gain vector, and the covariance matrix, respectively are,

$$\psi(t)= [-y(t-1)\ y(t-2)\ldots\ldots y(t-n_a)\ u(t-1)\ u(t-2)\ldots\ldots u(t-n_b)]^T$$

$$K(t) = \frac{P(t)\psi(t)}{\lambda(t) + \psi^T(t)P(t)\psi(t)} \qquad (6)$$

$$P(t+1) = \frac{1}{\lambda(t)}[P(t) - K^T(t)P(t)\psi(t)]$$

$\lambda(t)$ is the forgetting factor; n_a and n_b denote the order of the polynomials A and B, respectively. The identified parameters in (5) can be considered as the weighted sum of the previously identified parameters and those derived from the present signals.

4. The Control Strategy

Using the parameters obtained from the real time parameter identification method, a self-tuning controller based on pole assignment is computed on-line and fed to the plant. Under the pole shifting control strategy, the poles of the closed loop system are shifted radially towards the centre of the unit circle in the z-domain by a factor α, which is less than one. The procedure for deriving the pole–shifting algorithm [10] is given below.

Assume that the feedback loop has the form,

$$\frac{u(t)}{y(t)} = -\frac{G(z^{-1})}{F(z^{-1})} \qquad (7)$$

where,

$$F(z^{-1}) = 1+ f_1z^{-1} + f_2z^{-2} + f_3z^{-3} + f_4z^{-4} + \ldots\ldots\ldots\ldots +f_{nf}z^{-nf}$$

$$G(z^{-1}) = g_0+ g_1z^{-1} + f_2z^{-2} + f_3z^{-3} + f_4z^{-4} + \ldots\ldots\ldots +f_{ng}z^{-ng}$$

$$n_f = n_b-1,\ n_g = n_a-1$$

From (2) and (7) the characteristic polynomial can be derived as,

$$T(z^{-1})= A(z^{-1})F(z^{-1}) + B(z^{-1})G(z^{-1}) \qquad (8)$$

The pole-shifting algorithm makes $T(z^{-1})$ take the form of $A(z^{-1})$ but the pole locations are shifted by a factor α, i.e.

$$A(z^{-1})F(z^{-1}) + B(z^{-1})G(z^{-1}) = A(\alpha\ z^{-1}) \qquad (9)$$

Expanding both sides of (9) and comparing the coefficients give,

$$\begin{bmatrix} 1 & 0 & . & 0 & b_1 & 0 & . & 0 \\ a_1 & 1 & . & 0 & b_2 & b_1 & . & 0 \\ . & a_1 & . & . & . & b_2 & . & 0 \\ a_{n_a} & . & . & 1 & b_{n_b} & . & . & b_b \\ 0 & a_{n_a} & . & a_1 & 0 & b_{n_b} & . & b_2 \\ . & 0 & . & . & . & 0 & . & . \\ . & . & . & . & . & . & . & . \\ 0 & 0 & . & a_{n_a} & 0 & 0 & . & b_{n_b} \end{bmatrix} \begin{bmatrix} f_1 \\ . \\ . \\ f_{nf} \\ g_0 \\ . \\ . \\ g_{n_g} \end{bmatrix} = \begin{bmatrix} a_1(\alpha-1) \\ a_2(\alpha^2-1) \\ . \\ . \\ a_{n_a}(\alpha^{n_a}-1) \\ 0 \\ . \\ 0 \end{bmatrix}$$

The above is written in the form,

$$M\,Z(\alpha) = L(\alpha) \tag{10}$$

If parameters [{a_i}, {b_i}] are identified at every sampling period and pole-shift factor α is known, the control parameters Z=[{f_i},{g_i}}] solved from (10) when substituted in (7) will give,

$$u(t, \alpha) = X^T(t)Z = X^T(t)M^{-1}L(\alpha) \tag{11}$$

In the above, $X(t)=[-u(t-1)\ -u(t-2).....u(t-n_f)\ -y(t)\ -y(t-1)\ -y(t-2)..........y(t-n_g)]$

The controller objective is to force the system output y(t) to follow the reference output $y_r(t)$. The objective function can then be expressed as,

$$J = \min_{\alpha}[y(t) - y_r(t)]^2 \tag{12}$$

In the above, $y(t)=b_1u(t) + X^T\beta$; $\beta=[-b_2\ -b_3\ \ldots\ a_1\ a_2\ \ldots]$.

If the variation of J with respect to α can be made smaller than a predetermined error bound ε_1, it can be shown that a minimum of J will occur when,

$$\Delta\alpha = \frac{\varepsilon_1 - f_1 f_2}{\varepsilon_2 + \frac{1}{2}[f_1 f_3 + 2b_1^2 f_2^2]} \tag{13}$$

where, ε_2 is a small number chosen to avoid the singularity. In the above,

$$f_1 = \frac{\partial J}{\partial u};\quad f_2 = \frac{\partial u}{\partial \alpha};\quad f_3 = \frac{\partial^2 u}{\partial \alpha^2}$$

The partial derivatives are evaluated from (11) and (12), and updates of the control is obtained considering first few significant terms of the Taylor series expansion of $u(t,\alpha)$. The algorithm can be started by selecting an initial value of α and updating it at every sample through the relationship,

$$\alpha(t) = \alpha(t-1) + \Delta\alpha \tag{14}$$

The control function is limited by the upper and lower limits and the pole shift factor should be such that it should be bounded by the reciprocal of the largest value of characteristic root of A (z^{-1}). The latter requirement is satisfied by constraining the magnitude of α to unity.

5. Performance of Shunt Angle (α_E) Controller

The adaptive identification and control procedure was repeated for the power system given in Fig.1 considering the shunt converter voltage phase angle (α_E) of the UPFC as the input and the generator speed variation (Δω) as the output. The plant was excited by a sequence of torque pulses of +5%, -5%, +5%, and -5%, respectively. The initial covariance matrix, the initial value of the parameters, the initial value of the pole-shift factor (α), the forgetting factor and the model order were considered to be 2×10^5, .001, 0, 1 and 3, respectively.

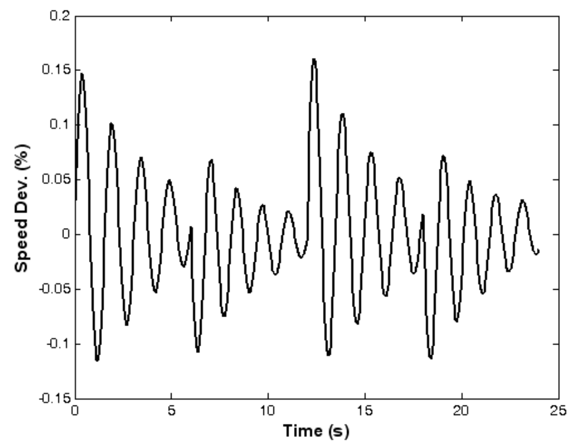

Figure 3 Generator speed variation with no control

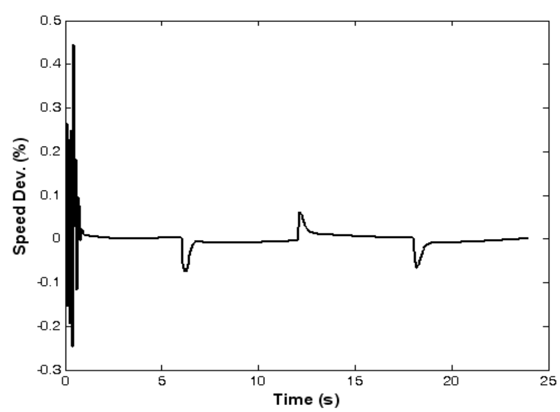

Figure 4 Generator speed deviation with the online adaptive stabilizing control

Fig.3 shows the generator speed deviation with no control when excited with the sequence of torque steps. The nominal loading is 0.85 pu at 0.9pf lagging. The generator terminal voltage at this load is 1.07 pu and the bus voltage is 1 pu. Fig.4 shows the variation of the generator speed with the pole-shift control applied to the identified process. As it can be observed, the system is stabilized very rapidly with the proposed adaptive pole-shift control. The plant parameters are unknown at the start of the estimation process which gives the poorer response in the early part of the transients. Fig. 5 shows the variation of the pole shift factor as the estimation procedure progresses. The convergence of the {a} and {b} parameters in the in the adaptive algorithm are shown in Figs. 6 and 7, respectively. The estimation algorithm converges to the desired values rapidly. The convergence of the algorithm is independent of the initial choice of the pole shift factor α.

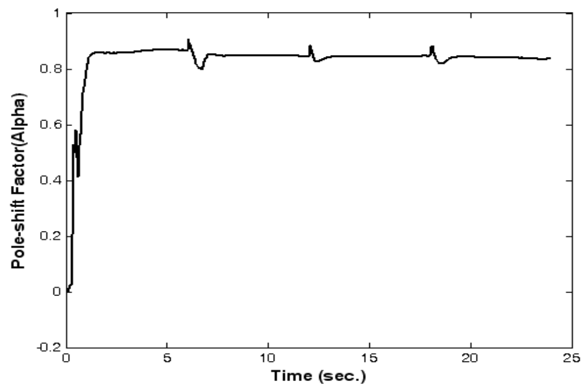

Figure 5 Online adaptation of the pole shift factor

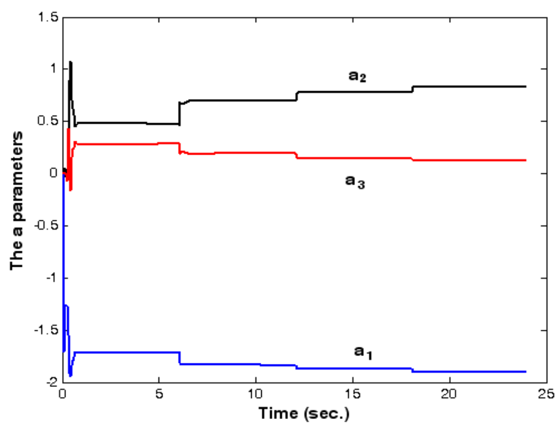

Figure 6 Online adaptations of the ‘a’ parameters in the model function

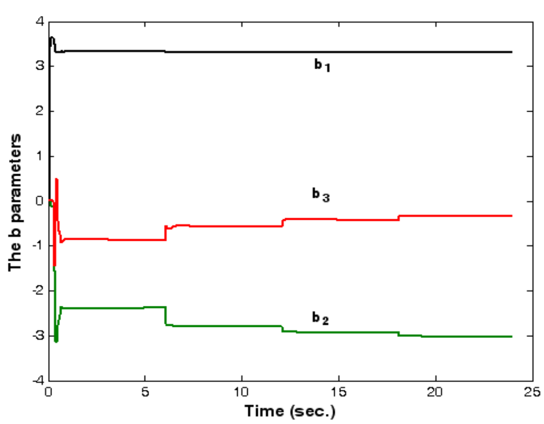

Figure 7 Online adaptations of the ‘b’ parameters

6. Testing the α_E Controller

A number of case studies were performed with the adapted and converged system parameters and the pole shift parameters. For a 100% input torque pulse on the generator, the rotor angle variations recorded for 5 operating conditions are shown in Fig.8. These are for generator outputs of a) 1.3 pu , b) 1.1 pu , c) 0.85pu , and, d) 0.62 pu. It can be observed that the damping properties are very good for the whole range of operation under consideration. These simulations were carried out with the converged plant model and pole-shift factor as obtained in the nominal loading considered in Figs. 4-7. In real applications, the models as well as the controls will be tuned on-line and is, hence, expected to provide better performance.

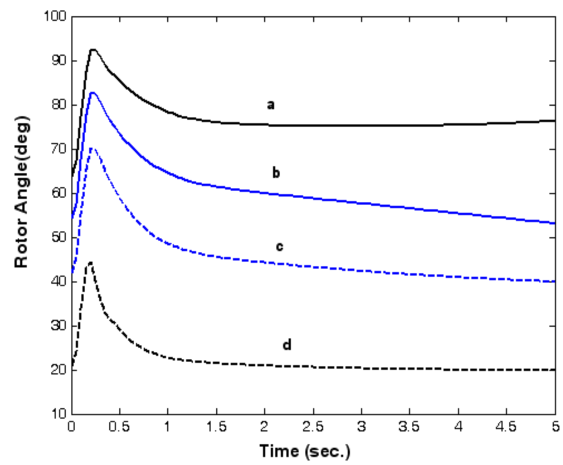

Figure 8 Generator rotor angle variations following 100% torque pulse for 5 loading conditions.

7. Evaluation of α_E with PI Control

The damping properties of the proposed coordinated robust controller were compared with a conventional PI controller in the shunt converter phase angle loop. The PI (or PID) controllers are normally installed in the feedback path. An additional washout is included in cascade with the controller to eliminate any unwanted signal in the steady state. The controller function in the feedback loop is written as,

$$H(s) = [K_P + \frac{K_I}{s}]\left[\frac{sT_w}{1+sT_w}\right] \qquad (15)$$

A pole–placement technique was used to determine the optimum gain settings (K_P and K_I) of the controller. For a desired location of the dominant closed-loop eigenvalue λ, the following equation is solved for K_P and K_I,

$$H(\lambda)= [C(\lambda I-A)^{-1}]^{-1} \quad (16)$$

$H(\lambda)$ is obtained from (15) for the desired λ .

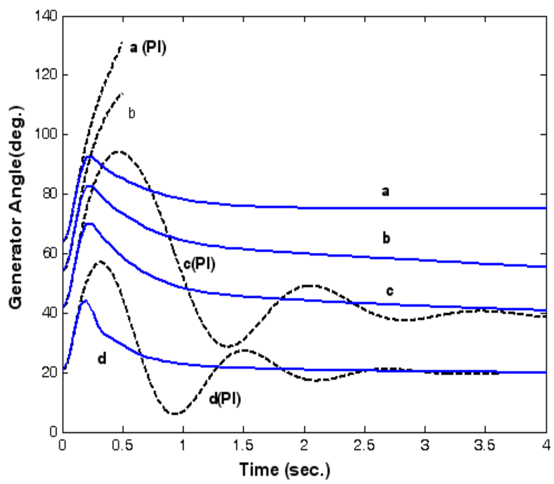

Fig. 9 Generator rotor angle characteristics following a 100% torque pulse of 0.1s for the 4 operating conditions with pole shift adaptive control (solid lines) and with PI controls (dotted lines).

Fig.9 shows the rotor angle variations of the synchronous generator with and without PI control for the 4 loading conditions considered in Fig.8. The nominal loading is 1.01 pu. The values of K_P and K_I, respectively are -11.8328 and 0.7715 for closed-loop system damping ratio of 0.3. The responses with dotted lines are with PI control. The disturbance considered is a 100% input torque pulse for 0.1s. The figure shows comparison of the responses of the PI control with the pole-shift adaptive control of shunt converter phase angle. It can be seen that for the operating conditions ‘a’ and ‘b’, the PI control is totally ineffective driving the system unstable. The pole-shift adaptive control, on the other hand, provides very well damped stable response for all the 4 operating conditions considered.

8. Performance and Evaluation of the Series Voltage Control

Adaptive stabilizing control of series converter voltage magnitude (m_B) was also attempted for the single machine system. The nominal loading condition and the disturbance considered are the same as considered in Fig. 3 of section 5. With the adaptive stabilizing control the angular speed variation of the generator is shown in Fig. 10.

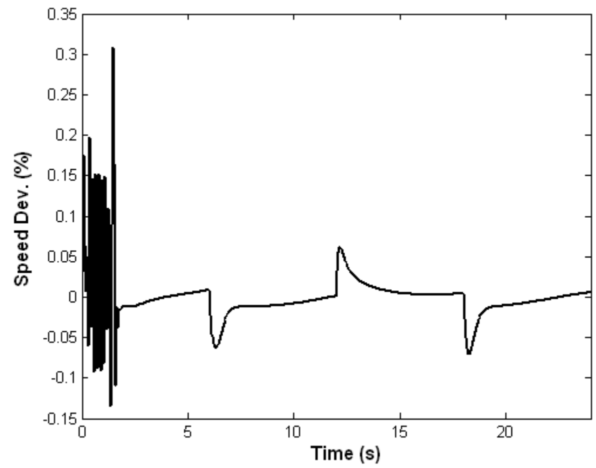

Figure 10 Generator speed variation corresponding to Fig.3 with adaptive pole-shift control

Fig. 11 shows the robustness of the controller tested for the 5 loading conditions of: a) 1.1 pu , b) 1.02 pu , c) 0.85pu , d) 0.78 pu, and e) 0.6pu with 50% torque pulse disturbance for 0.1s.

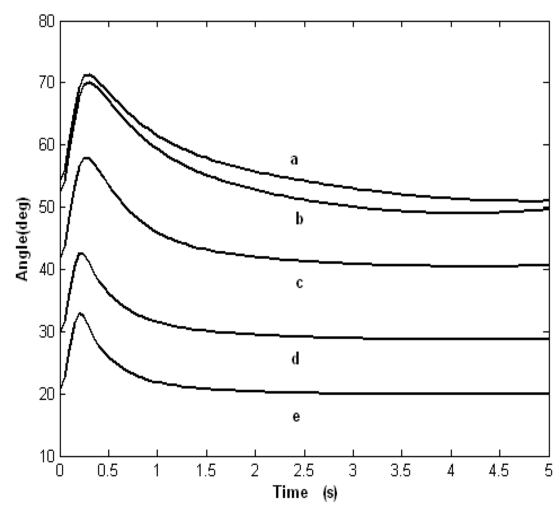

Fig. 11 Generator rotor angle variations following 50% torque pulse for 5 loading conditions.

A comparison of the adaptive series voltage control with the optimized PI control for three operating conditions: (a) 1.3, (b) 1.1, and (c) 0.45pu are shown in Fig. 12. It can be observed that while the PI control is satisfactory around the normal operating condition, for loadings like (a), it even fails to stabilize the system. The performance of the adaptive controller, on the other hand, is quite robust.

Though both shunt angle as well as series voltage controls can effectively damp the oscillations, a careful look will reveal that the shunt angle control is superior in terms of damping profiles for same loading conditions.

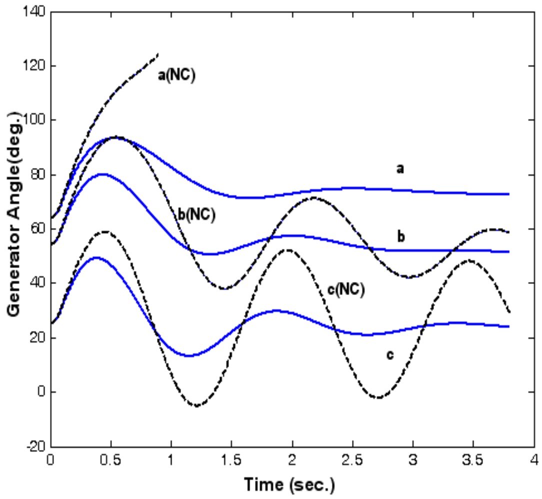

Fig.12 Generator rotor angle variations for a 50% torque pulse disturbance of 0.1s for three different operating conditions a, b and c with and without (NC) PI control.

9. Conclusion

An adaptive control technique has been employed to enhance the dynamic performance of a power system installed with unified power flow controller. Responses with control of both the shunt converter phase angle and series converter voltage magnitude have been compared. While both the adaptive strategies provide good damping for the transients, the phase angle control was observed to be slightly superior. The algorithms have been shown to converge to estimated parameter model rapidly. The robustness of the control strategy was tested by considering the converged values obtained from the test phase. The adaptive strategies were applied to a range of operating conditions and were observed to provide robust performance over the whole range. The strategies were much superior to the PI controls with optimized gain settings.

Acknowledgement

The authors wish to acknowledge the facilities provided by the King Fahd University of Petroleum and Minerals towards this research.

References

[1] L. Gyugyi, "A Unified Power Flow Control Concept for Flexible AC Transmission Systems", *IEE Proceedings* – C, vol. 139, No. 4. pp. 323 – 331, July 1992.

[2] L. Gyugyi, C. D. Schauder, S. L. Williams, T. R. Rietman, D. R. Torgerson, A. Edris, "The Unified Power Flow Controller: A new approach to power transmission control", *IEEE Transactions on Power Delivery*, vol. 10, No. 2, pp. 1085-1093, April, 1995.

[3] Seo, J., Moon, S., Park, J. and Choe, J., "Design of a Robust UPFC Controller for Enhancing the Small Signal Stability in the Multi-machine Power Systems", *IEEE Power Engineering Society Winter Meeting,* 2001, Vol. 3, pp.1197-1202.

[4] Wang, H.F., "Damping Function of Unified Power Flow Controller", *IEE Proc.-Gener. Transm. Distrib.*, 1999, 146(1), pp.81-87.

[5] Tambey, N. and Kothari, M.L., "Damping of Power System Oscillations with Unified Power Flow Controller (UPFC)", *IEE Proc.-Gener. Transm. Distrib.,* 2003, 150(2), pp.129-140.

[6] Wu, X., Qu, Z., and Mohapatra, R.N., "Stability Constrained Operation of UPFC Devices", *IEEE Transmission& Distribution Conference & Exposition*, 2001, Vol. 1, pp.31-36.

[7] Wang, H.F., "Applications of Modeling UPFC into Multi-machine Power Systems", *IEE Proc.-Gener. Transm. Distrib.*, 1999, 146(3), pp.306-312.

[8]W.M.Hussein and O.P.Malik, "Study of System Performance with Duplicate Adaptive Power System Stabilizer", *Electric Power Components and Systems*, 2003, 31, 899-912.

[9] J.R. Smith, D.A. Pierre , D.A.Rudberg, I. Sadhigi, A.P.Johnson and J.F.Hauer, An Enhanced LQ Adaptive VAr Unit Controller for Power System Damping, *IEEE Trans. on Power Systems*, 1989, 4(2), 443-451.

[10]O.P.Malik, G.P.Chen, G.S. Hope, Q.H.Qin and G.Y.Xu, "Adaptive Self-optimizing Pole Shifting Control Algorithm", *IEE Proc.-D,* 1992, 139(5), 429-438.